LA-UR-15-20779 (Accepted Manuscript)

Simultaneous /2 rotation of two spin species of different gyromagnetic ratios

Chu, Pinghan
Peng, Jen-Chieh

Provided by the author(s) and the Los Alamos National Laboratory (2016-04-05).

To be published in: Nuclear Instruments and Methods in Physics Research Section A: Accelerators, Spectrometers, Detectors and Associated Equipment

DOI to publisher's version: 10.1016/j.nima.2015.05.062

Permalink to record: http://permalink.lanl.gov/object/view?what=info:lanl-repo/lareport/LA-UR-15-20779

Disclaimer:
Approved for public release. Los Alamos National Laboratory, an affirmative action/equal opportunity employer, is operated by the Los Alamos National Security, LLC for the National Nuclear Security Administration of the U.S. Department of Energy under contract DE-AC52-06NA25396. Los Alamos National Laboratory strongly supports academic freedom and a researcher's right to publish; as an institution, however, the Laboratory does not endorse the viewpoint of a publication or guarantee its technical correctness.

arXiv:1505.06406v1 [nucl-ex] 24 May 2015

Simultaneous $\pi/2$ rotation of two spin species of different gyromagnetic ratios

Ping-Han Chu[a,b,*], Jen-Chieh Peng[b]

[a] *Triangle Universities Nuclear Laboratory and Department of Physics, Duke University, Durham, North Carolina 27708, USA*

[b] *Department of Physics, University of Illinois at Urbana-Champaign, Urbana, Illinois 61801, USA*

Abstract

We examine the characteristics of the $\pi/2$ pulse for simultaneously rotating two spin species of different gyromagnetic ratios with the same sign. For a $\pi/2$ pulse using a rotating magnetic field, we derive the equation relating the frequency and strength of the pulse to the gyromagnetic ratios of the two particles and the strength of the constant holding field. For a $\pi/2$ pulse using a linear oscillatory magnetic field, we obtain the solutions numerically, and compare them with the solutions for the rotating $\pi/2$ pulse. Application of this analysis to the specific case of rotating neutrons and ^{3}He atoms simultaneously with a $\pi/2$ pulse, proposed for a neutron electric dipole moment experiment, is also presented.

Keywords:
$\pi/2$ rotation, magnetic resonance, neutron electric dipole moment

The $\pi/2$ rotation is a commonly used technique in nuclear magnetic resonance. A spin $\vec{S}$ with a gyromagnetic ratio γ, pointing along a constant magnetic field B_0 in the $\hat{z}$ direction, can be rotated into the $\hat{x}-\hat{y}$ plane by applying a radio-frequency (rf) magnetic field $\vec{B}(t)$, called a $\pi/2$ pulse, in the direction orthogonal to B_0. For a $\pi/2$ pulse rotating in the $\hat{x}-\hat{y}$ plane, $\vec{B}(t)$

*Present address: Los Alamos National Lab, P.O. Box 1663, H803, Los Alamos, NM, 87544, USA. Tel.: +1 5056060510

Email address: pchu@lanl.gov (Ping-Han Chu)

can be written as

$$B_x(t) = B_1 \sin(\omega_{rf} t),\ B_y(t) = B_1 \cos(\omega_{rf} t), \tag{1}$$

which represents a magnetic field with frequency ω_{rf} and an amplitude B_1. While ω_{rf} is often chosen to be the same as the resonant Larmor frequency, $\omega_0 = \gamma B_0$, off-resonance frequencies could also be used. As discussed below, this capability to perform a $\pi/2$ rotation with off-resonance frequencies makes it possible to rotate simultaneously two spin species of different gyromagnetic ratios with a single $\pi/2$ pulse of suitable frequency and duration.

The need to rotate two different spin species with a single $\pi/2$ pulse is relevant for the proposed experiment [1, 2, 3] at the Oak Ridge National Laboratory to search for the neutron electric dipole moment (EDM) using polarized ultra-cold neutrons stored in a superfluid helium cell containing polarized ^{3}He acting as a co-magnetometer and a spin-analyzer. A non-zero neutron EDM can be observed by measuring the difference of the precession frequencies of neutrons when electric and magnetic fields are aligned or anti-aligned. The initial polarization directions for neutron and ^{3}He spins are parallel to a constant B_0 field pointing along the $\hat{z}$ axis. To measure the precession frequency of neutrons relative to that of ^{3}He, a single $\pi/2$ pulse will be applied to rotate both spins into the $\hat{x} - \hat{y}$ plane. A superconducting quantum interference devices (SQUID) will be used to measure the precession frequency of ^{3}He [4], and the relative precession between neutrons and ^{3}He can be determined by the rate of the absorption reaction, n + ^{3}He $\rightarrow$ p + ^{3}H, which depends sensitively on the relative spin orientations of neutrons and ^{3}He [5]. From the measurements of the precession of ^{3}He and the absorption reaction of n-^{3}He, the precession frequency of neutrons can be determined. An alternative method, the dressed spin technique, could also be used to measure the neutron EDM by applying an additional dressing field [1, 6].

It is not evident that two spin species with different gyromagnetic ratios could be rotated simultaneously by a $\pi/2$ pulse. As shown in this paper, this is only possible if the ratio of the magnetic moments of the two spin species falls within a certain range. Vasserman et al. utilized a method to simultaneously rotate the spins of electron and positron by 90° to measure their anomalous magnetic moments for a test of CPT invariance [7]. This method is only applicable for particles with identical magnitude of gyromagnetic ratios. Recently, de Lange et al. published a new method to manipulate two spin species using the spin echo technique [8]. However, this method requires

a spin bath which does not exist in many experiments such as the neutron EDM experiment. It is necessary to consider other methods which do not require a spin bath. The purpose of this paper is to discuss a method which is generally applicable to experiments requiring a simultaneous $\pi/2$ rotation for two different spin species.

The rest of this paper is organized as follows. First, we derive the equations for calculating ω_{rf} and τ as a function of B_0, B_1, and the gyromagnetic ratios of two different spin species. Second, we explore the range of these parameters and the relation between them. Third, we present the numerical solutions and comment on the characteristics of the solutions. Finally, we also consider the case for linear rf magnetic fields, which are more readily implemented than rotating fields, and compare the solutions with those of rotating rf fields. The application of this study to the specific case of the neutron EDM experiment involving neutron and ^{3}He will also be presented. Some initial results obtained by one of the coauthors (JCP) for the case of rotating rf fields were presented in an unpublished report [2].

In general, the spin motion of polarized particles moving in an external electromagnetic field can be described by the Bargmann-Michel-Telegdi equation [9]. However, for non-relativistic particles, the dynamics of a spin in a magnetic field system can be described by the Bloch equation [10]:

$$\frac{d\vec{S}}{dt} = \vec{S} \times (\gamma \vec{B}(t)). \tag{2}$$

Here we consider a system of polarized particles moving slowly in a cell with a static magnetic field, B_0, parallel to the spin orientation of polarized particles along the $\hat{z}$-axis. Upon the application of the rotating field given in Eq. 1, the effect on the spin direction of the particles can be conveniently described by transforming to a frame rotating at ω_{rf} along $\hat{z}$. In this rotating frame with axes defined by the $\hat{x}', \hat{y}'$, and $\hat{z}'$ as shown in Fig. 1, the field $\vec{B}(t)$ becomes static with a magnitude B_1 pointing along the $\hat{y}'$ axis. The static B_0 field in the $\hat{z}'$ axis is changed to $B_0 - \omega_{rf}/\gamma$ in this rotating frame and the spins of the particles will precess about the magnetic field $\vec{B}_{tot}$ given as

$$\vec{B}_{tot} = (B_0 - \frac{\omega_{rf}}{\gamma})\hat{z}' + B_1\hat{y}' \tag{3}$$

with an effective Larmor frequency

$$\omega_0' = \gamma\sqrt{(B_0 - \frac{\omega_{rf}}{\gamma})^2 + B_1^2}. \tag{4}$$

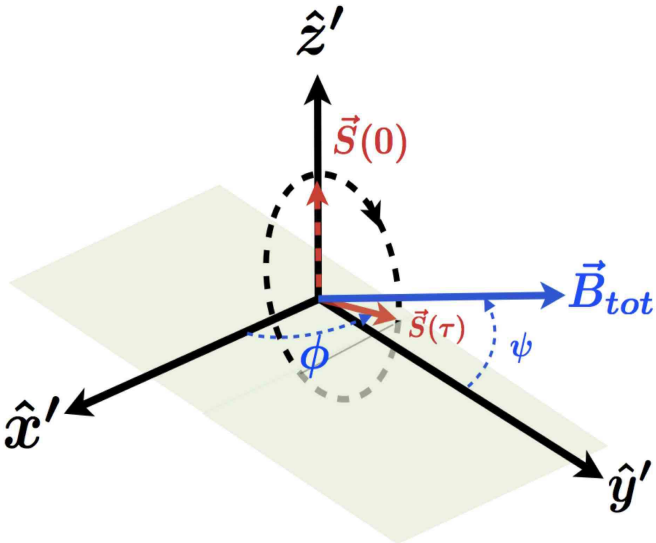

Figure 1: (Color figure) Schematic plot of spin rotation using a rotating rf field $B_1(t)$ in the $\hat{x}-\hat{y}$ plane with frequency ω_{rf}. The holding field B_0 is along $\hat{z}$-axis. In a frame rotating at ω_{rf} along $\hat{z}$, the effective field is $\vec{B}_{tot} = (B_0 - \frac{\omega_{rf}}{\gamma})\hat{z}' + B_1\hat{y}'$. $\vec{S}(0)$ is the initial spin orientation and $\vec{S}(\tau)$ is the spin orientation after applying a $\pi/2$ pulse. ψ is the angle between $\vec{B}_{tot}$ and $\hat{y}'$ and ϕ the angle between $\vec{S}(\tau)$ and $\hat{x}'$.

The angle ψ between the directions of $\vec{B}_{tot}$ and $\hat{y}'$ satisfies

$$\tan\psi = \frac{B_0 - \omega_{rf}/\gamma}{B_1} = \frac{B_0}{B_1}(1 - \frac{\omega_{rf}}{\gamma B_0}). \tag{5}$$

It is convenient to define another coordinate system ($\hat{x}''$, $\hat{y}''$, $\hat{z}''$) obtained from a rotation along the $\hat{x}'$ axis by an angle ψ such that $\hat{y}''$ is along the direction of $\vec{B}_{tot}$:

$$\begin{bmatrix} \hat{x}'' \\ \hat{y}'' \\ \hat{z}'' \end{bmatrix} = \begin{bmatrix} 1 & 0 & 0 \\ 0 & \cos\psi & \sin\psi \\ 0 & -\sin\psi & \cos\psi \end{bmatrix} \begin{bmatrix} \hat{x}' \\ \hat{y}' \\ \hat{z}' \end{bmatrix}. \tag{6}$$

The spin of the particle is initially along the $\hat{z}'$-axis. At a later time t, it can be expressed as

$$\vec{S}(t) = \vec{S}_{\parallel}(t) + \vec{S}_{\perp}(t), \tag{7}$$

where $\vec{S}_{\parallel}(t)$ is the component parallel to $\vec{B}_{tot}$ and is independent of time,

$$\vec{S}_{\parallel}(t) = |\vec{S}| \sin\psi \hat{y}''. \tag{8}$$

$\vec{S}_{\perp}$ is the component perpendicular to $\vec{B}_{tot}$ and will rotate about $\vec{B}_{tot}$ so that

$$\vec{S}_{\perp}(t) = (|\vec{S}| \cos\psi)(\cos(\omega_0' t)\hat{z}'' - \sin(\omega_0' t)\hat{x}''). \tag{9}$$

Using Eqs. 6- 9, $\vec{S}(t)$ can be expressed in terms of the coordinates in the rotating frame as

$$\begin{aligned}\vec{S}(t) &= \vec{S}_{\parallel}(t) + \vec{S}_{\perp}(t) \\ &= |\vec{S}|(\sin\psi)\hat{y}'' + (|\vec{S}|\cos\psi)(\cos(\omega_0' t)\hat{z}'' - \sin(\omega_0' t)\hat{x}'') \\ &= |\vec{S}|[-\cos\psi \sin(\omega_0' t)\hat{x}' + \sin\psi\cos\psi(1-\cos\omega_0' t)\hat{y}' \\ &+ (\sin^2\psi + \cos^2\psi\cos\omega_0' t)\hat{z}'].\end{aligned} \tag{10}$$

For an rf pulse to rotate the spin from the vertical axis to the horizontal plane after a duration τ, the component of $\vec{S}(\tau)$ along $\hat{z}'$ must vanish:

$$\vec{S}(\tau)\cdot\hat{z}' = \sin^2\psi + \cos^2\psi\cos\omega_0'\tau = 0. \tag{11}$$

We can readily obtain the solutions for ω_{rf} and τ to rotate two spin species of different gyromagnetic ratios by $\pi/2$ simultaneously. Due to the property of the cos function, the sign of ω_0' does not change the solution of τ; this implies the solution of τ is suitable for both positive and negative ω_0' as well as γ. Denoting the gyromagnetic ratios for the two spin species as γ_1 and γ_2, and their Larmor frequencies as $\omega_{0,1} = \gamma_1 B_0$ and $\omega_{0,2} = \gamma_2 B_0$, the requirement is to have the same duration, τ, with a given frequency to simultaneously rotate both species by $\pi/2$. Therefore, we obtain:

$$\tau = \frac{\cos^{-1}(-\tan^2(\psi_1))}{|\omega_{0,1}'|} = \frac{\cos^{-1}(-\tan^2(\psi_2))}{|\omega_{0,2}'|} \tag{12}$$

where $\omega_{0,i}'$ and ψ_i are the effective Larmor frequency and ψ angle for species i in Eq. 4 and Eq. 5, respectively. The range of $\cos^{-1}(-\tan^2(\psi))$ is from 0 to π in order to keep τ positive.

The solutions for ω_{rf} must also satisfy the following constraint:

$$-1 \leq \tan\psi_i \leq 1,$$

i.e.

$$-1 \leq (\frac{B_0}{B_1})(1 - \frac{\omega_{rf}}{\gamma_i B_0}) \leq 1, \tag{13}$$

implying

$$1 - \frac{B_1}{B_0} \leq \frac{\omega_{rf}}{\gamma_i B_0} \leq 1 + \frac{B_1}{B_0}. \tag{14}$$

It is also noted that after the application of a $\pi/2$ pulse, the spin directions of the two species on the $\hat{x} - \hat{y}$ plane would in general be different. Using Eqs. 10 and 11, the azimuthal angle ϕ_i of the spin for species i after a $\pi/2$ rotation is given as

$$\phi_i = \tan^{-1}(\frac{\sin\psi_i \cos\psi_i (1 - \cos\omega'_{0,i}\tau)}{-\cos\psi_i \sin\omega'_{0,i}\tau}) = -\tan^{-1}(\frac{1}{\sqrt{\cot^2\psi_i - 1}}). \tag{15}$$

Therefore, the spins of the two species are usually not aligned ($\phi_1 \neq \phi_2$) right after the $\pi/2$ pulse.

Equation 12 can be solved numerically to find ω_{rf} for given values of B_0, B_1, and γ_i. Because the gyromagnetic ratios of neutron and ^{3}He are both negative, we focus on the case of both spin species having gyromagnetic ratios of the same sign in this paper. We note that Eq. 12 is also applicable for the case of two spin species having gyromagnetic ratios of opposite signs. For convenience, we define dimensionless parameters if both gyromagnetic ratios are in the same sign: $R = \frac{\gamma_1}{\gamma_2}$, $x = \frac{B_0}{B_1}$ and $y = \frac{2\omega_{rf}}{\omega_{0,1}+\omega_{0,2}}$. Fig. 2(a) shows the solutions for y as a function of x for three different values of R. We only consider the case for $R \geq 1$, since the $R \leq 1$ case simply corresponds to interchanging the two spin species. We first note that for a given value of R ($R \equiv \gamma_1/\gamma_2$), a solution for ω_{rf} can be found only within a certain range of x. This range becomes narrower as R increases, and above certain value of R, there is no longer a solution for ω_{rf}. The domain in R versus x for which a solution for ω_{rf} exists is shown as the red region in Fig. 2(b).

Figure 2(a) also shows that the solutions for y at different values of R have very similar shapes. It is interesting to study the phenomena when R approaches 1 (but not equal to 1). Inserting $R \approx 1 + \delta R$ into Eq. 12 and

ignoring higher-order terms in δR, the solution for y versus x when $R \to 1$ is

$$\begin{aligned} &\cos^{-1}(x^2(-1+y)^2) \\ =&\pi - \frac{2(x^2y(1-y))}{1+x^2(1-y)}\sqrt{\frac{1+x^2(1-y)^2}{1-x^2(1-y)^2}}, \end{aligned} \tag{16}$$

shown as the black-dashed curve in Fig. 2(a). However, when $R = 1$, corresponding to the degenerate case of a $\pi/2$ rotation for only a single species, the solution is given by Eq. 14, shown as the yellow region in Fig. 2(a). This abrupt change from a curve to a band for the solution of Eq. 12 reflects the degeneracy occurring at $R = 1$.

The solution for the specific case of rotating neutron and ^{3}He simultaneously with a $\pi/2$ pulse, relevant for a proposed neutron EDM experiment [2], is shown in Fig. 3. The black-dashed curve in Fig. 3(a) gives the solution for y versus x at $R = \gamma_3/\gamma_n = 1.1121$, where n and 3 represent neutron and ^{3}He, respectively. Figure 3(b) and (c) also show solutions of the duration τ from Eq. 12 and the angular difference of spins of two species after a $\pi/2$ rotation, $\Delta\phi_{n3} = \phi_n - \phi_3$, from Eq. 15. Also shown in Fig. 3 are the solutions for linear rf fields, to be discussed next.

The study so far assumes a rotating rf field. However, a linear rf field is commonly utilized in experiments due to its simplicity to implement. Therefore, we extend our study to the case of a linear rf field, which can be decomposed in terms of two rotating components:

$$\begin{aligned} B_{rf}(t) &= 2B_1\cos(\omega_{rf}t)\hat{y} \\ &= B_1(\sin(\omega_{rf}t)\hat{x} + \cos(\omega_{rf}t)\hat{y}) + B_1(-\sin(\omega_{rf}t)\hat{x} + \cos(\omega_{rf}t)\hat{y}) \end{aligned} \tag{17}$$

The first component corresponds to the rotating field we have considered, which is stationary in the rotating frame. The second component rotates with a frequency of $-2\omega_{rf}$ in the rotating frame. To assess the effect of this high frequency term, we have solved the time dependence of $\vec{S}$ numerically using the Bloch equation (Eq. 2). We have considered the specific case for neutron and ^{3}He with the gyromagnetic ratio -18.32472 and -20.37895 Hz/mG, respectively, and with B_0 at 10 mG. The Runge-Kutta method is applied and the time step of the simulation is $\Delta t = 10^{-6}$ sec. In order to determine a single $\pi/2$ pulse for both neutron and ^{3}He, the following algorithm is applied. Initially, both neutron and ^{3}He spins are along the $\hat{z}$-axis. Using the numerical simulation of the Bloch equation for a given $x = \frac{B_0}{B_1}$ and

$y = \frac{2\omega_{rf}}{\omega_{0,1}+\omega_{0,2}}$, we derive the duration τ when the neutron spin is rotated into the $\hat{x} - \hat{y}$ plane, i.e., the $\hat{z}$-component of the neutron spin becomes zero. In practical terms we derive the duration when the $\hat{z}$-component of the neutron spin changes its sign, from a positive value to a negative value. Although the spin is wobbling, we just use the first point when the neutron spin is rotated into the $\hat{x} - \hat{y}$ plane. Then, at τ, we consider the difference of the $\hat{z}$-component between the spins of neutron and ^{3}He. For a given $x = \frac{B_0}{B_1}$, we vary $y = \frac{2\omega_{rf}}{\omega_{0,1}+\omega_{0,2}}$ until the difference of the $\hat{z}$-component between the spins of neutron and ^{3}He changes sign. Using this algorithm, we can derive the solutions of the linear rf fields for the simultaneous $\pi/2$ rotation of neutron and ^{3}He.

Fig. 4 shows an example of a $\pi/2$ pulse for neutron and ^{3}He using a linear rf field. The vertical components of the spins of the two species as a function of time are shown as red-solid and green-dotted curves for neutron and ^{3}He, respectively. The oscillatory pattern in these two curves has a frequency of $\sim 2\omega_{rf}$. Fig. 4 shows that the both spins can be simultaneously rotated to the $\hat{x} - \hat{y}$ plane with the linear rf field.

In Fig. 3(a), the solutions using the Bloch equation are shown for both rotating and linear rf fields. Significant difference between the two cases is observed for smaller values of B_0/B_1. At large values of B_0/B_1, the effect of the high-frequency counter rotating term could be neglected. The time duration τ and the angular difference after $\pi/2$ pulses for $R = \gamma_3/\gamma_n$ are also shown in Fig. 3(b) and (c). They show that the results of the time duration in Eq. 12 and the angular difference in Eq. 15 are consistent with those of numerical simulation using Bloch equation for rotating rf fields. The results for linear rf fields follow those for rotating rf fields, but with an oscillatory pattern superimposed.

In summary, we have studied the solutions for $\pi/2$ pulses for two spin species of the same-sign gyromagnetic ratios using rotating and linear rf fields. The characteristics of the solutions are presented. For a specific experiment, the selection of the optimal values of B_0, B_1 could depend on various considerations. This study provides the solution for ω_{rf}, once the values of B_0, B_1 are chosen. The application of this work to a neutron EDM experiment [2] is also discussed. Finally, this study can be extended to the case of two spin species having gyromagnetic ratios of opposite signs.

We gratefully acknowledge valuable discussions with Bradley W. Filippone and Riccardo Schmid. This work was supported by the U.S. National

Science Foundation and the Department of Energy.

References

[1] R. Golub and S. K. Lamoreaux, *Phys. Rept.*, **237**, 1 (1994).

[2] D. Budker et al., A New Search for the Neutron Electric Dipole Moment, *Los Alamos National Laboratory Tech. Rep.* **LA-UR 02-2331** (2002).

[3] T. M. Ito, *J. Phys. Conf. Ser.*, **69** 012037 (2007).

[4] Y. J. Kim and S. M. Clayton, *IEEE Trans. Appl. Supercond.* **23**, 2500104 (2013).

[5] L. Passel and R. I. Schermer, *Phys. Rev.* **150**, 146 (1966).

[6] P.-H. Chu et al., *Phys. Rev.* C **84**, 022501 (2011).

[7] I. B. Vasserman et al., Phys. Lett. B **198**, 302 (1987)

[8] G. de Lange et al., *Sci. Rep.* **2**, 382 (2012).

[9] V. Bargmann, L. Michel and V. L. Telegdi, *Phys. Rev. Lett.*, **2**, 435 (1956).

[10] F. Bloch, *Phys. Rev.*, **70**, 460 (1946).

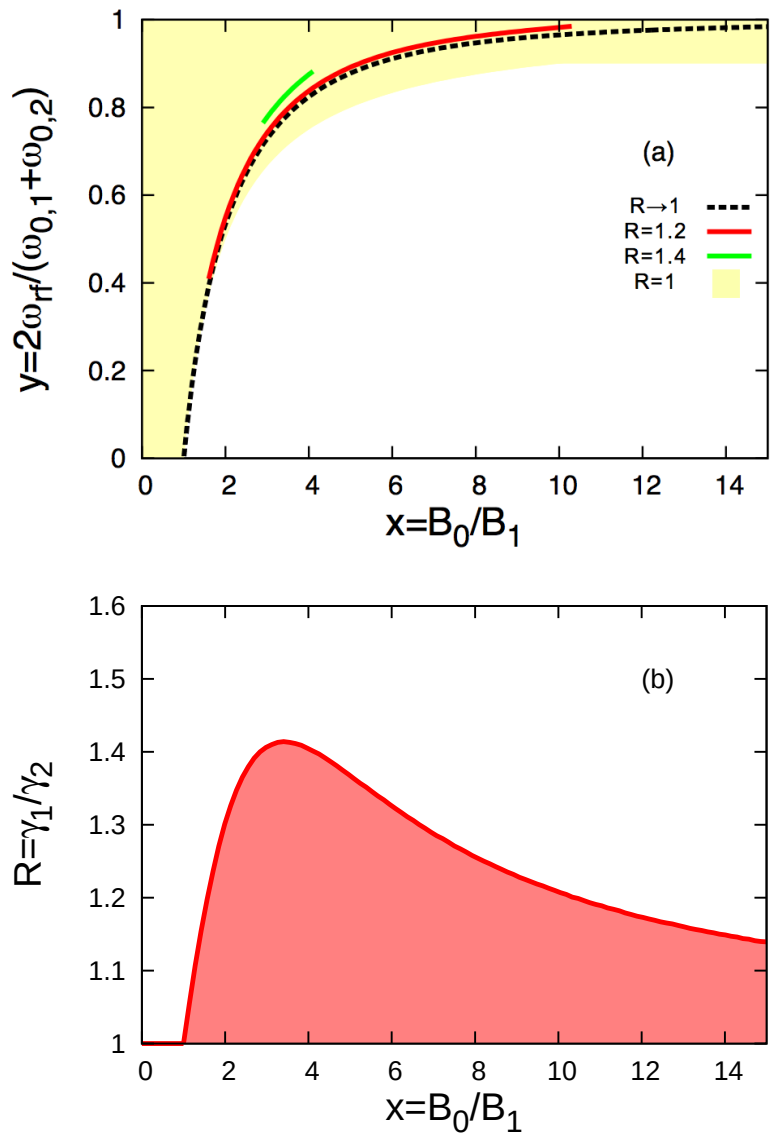

Figure 2: (Color figure) Solutions of the $\pi/2$ rotation for two spin species. (a) $y = 2\omega_{rf}/(\omega_{0,1}+\omega_{0,2})$ versus $x = B_0/B_1$ for different $R = \gamma_1/\gamma_2$. The yellow region shows the constraint of the $\pi/2$ rotation for a single spin species according to Eq. 14. (b) $R = \gamma_1/\gamma_2$ versus $x = B_0/B_1$. All values in the red region can be used for $\pi/2$ pulses.

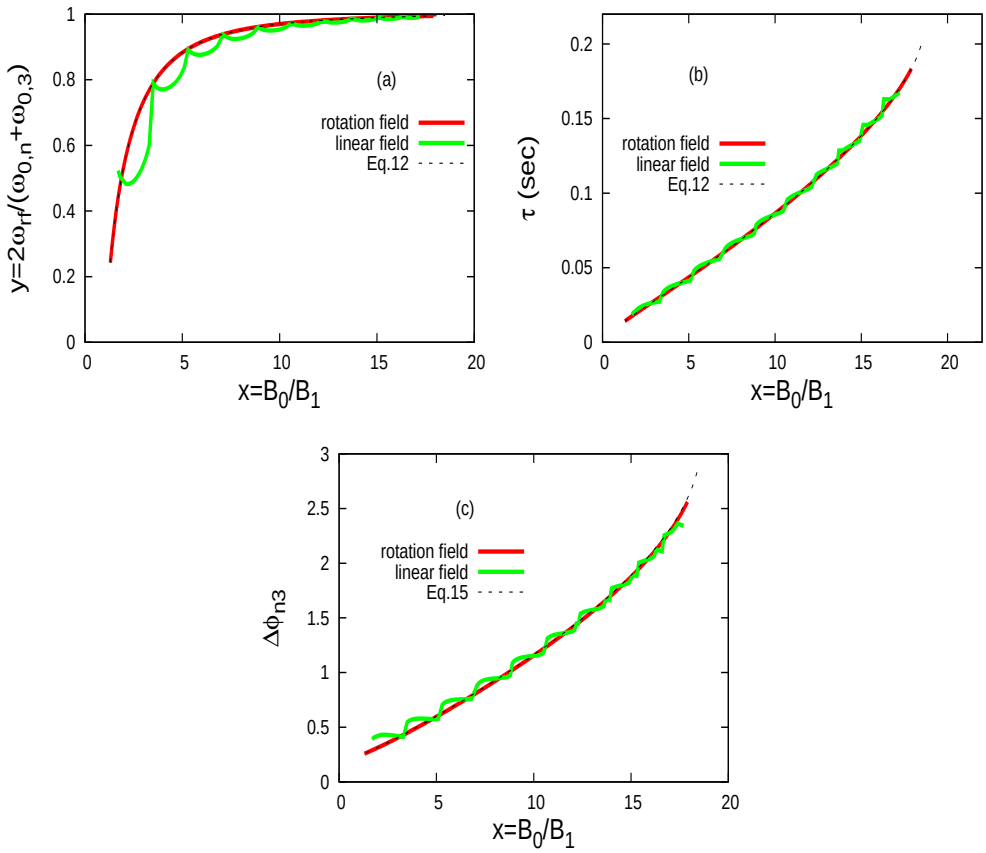

Figure 3: (Color figure) Solutions of the $\pi/2$ pulses for neutron and ^{3}He, i.e., $R = \gamma_3/\gamma_n$. The holding field B_0 is 10 mG along the z-axis. (a) $y = 2\omega_{rf}/(\omega_{0,1} + \omega_{0,2})$ versus $x = B_0/B_1$. (b) Time duration τ versus B_0/B_1. (c) The angular difference, $\Delta\phi_{n3}$, between spins of neutron and ^{3}He after the $\pi/2$ pulses. The black-dashed curves and the red-solid curves are solutions for rotating rf fields using the analytical equations (Eqs. 12 and 15) and the Bloch equation, respectively. The results from these two approaches are identical. The green-dotted curves are obtained using Bloch equation simulation with linear rf fields.

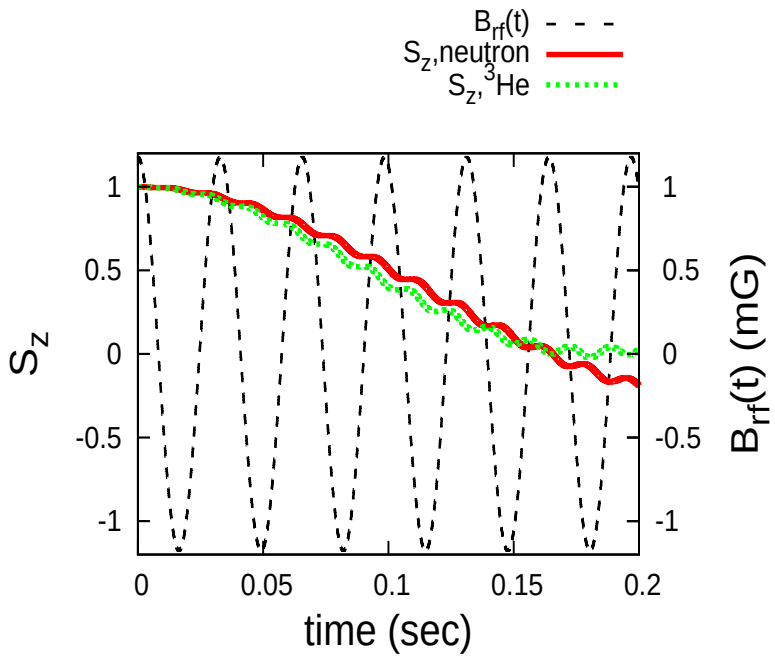

Figure 4: (Color figure) The time dependence of S_z for neutron and ^{3}He with a linear rf field. The red-solid and green-dotted curves are neutron and ^{3}He, respectively. B_0 is 10 mG along the $\hat{z}$-axis, and the black-dashed curve shows the amplitude and frequency of the linear rf field, $B_{rf}(t)$, defined in Eq. 17. ($x = B_0/B_1 = 17$, $y = \frac{2\omega_{rf}}{\omega_{0,1}+\omega_{0,2}} = 0.989596$)